Rev. Roum. Sci. Techn.– Électrotechn. et Énerg.
Vol. **68**, *2*, pp. 152–157, Bucarest, 2023

ENERGY CONSUMPTION ANALYSIS FOR AN EV POWERTRAIN USING THREE BRUSHLESS DC IDENTICAL MOTORS

LIVIU POPESCU[1], OVIDIU CRAIU[2]

Keywords: Permanent magnet (PM) motors; Electric vehicles (EV); Multi-motor powertrain; Efficiency maps.

Using more than one motor in an EV (Electric Vehicle) powertrain enhances the vehicle's torque, acceleration, and speed capabilities. A more tractive force produced by the electric powertrain requires more electric current from the battery. In modern EVs, mechanical power production can be approached to the wheels reducing the mechanical losses in the transmissions. It is the case with multiple-motor powertrains. Several advantages regarding vehicle control, physical performance, and energy efficiency improvement are obtained. In the current study, a BLDC (brushless dc) motor is investigated from the efficiency point of view to build a multiple-motor powertrain. A new methodology uses analytic calculations, simulations, and physical measurements. A powertrain with three identical motors results in a new vehicle configuration. Each motor's energy consumption improvements are analyzed following a normalized testing procedure. The results are compared with those of a single-motor powertrain.

1. INTRODUCTION

More mobility possibilities are increasingly based on electric vehicles (EVs) [1]. Such solutions are not often used but could become mainstream, as the technology is already there [2,3]. One of the main advantages is the possibility of constituting multi-motor powertrains [4], improving energy efficiency, and searching for better control [5] and optimization [6]. Therefore, the architecture of new vehicles should be adapted to integrate multiple electric motors [7,8]. Future specialized engineers must be formed to conceive such systems [9]. The efficiency of the electric motors is in the middle of the efficiency chain of the EV powertrains. Diverse research continues to find solutions for better performance [10–19]. In the actual analysis, the method presented in [20] is detailed in a new specific case of efficiency maps constitution, continuing the experience in previous research [21–24].

A BLDC (brushless dc) motor is investigated to contribute to a multi-motor powertrain. Precedent studies showed that applying phase advance and dwell control [25] and different control methods [26–28] can improve the BLDC performance, mainly increasing the motor efficiency and its no-load speed. Approaching the production of mechanical power to the wheels, using multiple motors, can generate efficiency and performance [29]. But the optimal repartition of the torque between multiple motors [30–33] represents a question of vehicle stability [34]. Therefore, the power distribution among electric motors and the powertrain efficiency remain important in designing mobility solutions [36,37]. The current investigation is based on precedent experiences in simulation [38] and experimental measurements [9]. Several methods can be used to control energy efficiency [39,40]. Based on previous investigations [41], a similar BLDC motor is analyzed from the efficiency maps' point of view. Then, a three-identical motor powertrain is proposed and analyzed to power an EV with an increased mass.

As mentioned before, it is important to approach the motors to the wheels. In the new configuration, the vehicle has two motors operating individually on each rear wheel and another on the front axle. The efficiency maps from [20] analyze each motor's contribution to the mechanical power supplied to the wheels. A specific procedure integrating analytic calculations, simulations, and physical measurements is used to analyze the three-motor powertrain.

A normalized testing cycle is used as a speed profile for the investigations. The most demanding area of the speed profile, the high-speed zone, has been chosen for measuring the powertrain performance in the case of using one motor and, respectively when using three motors. An optimal load distribution is compared to a static load distribution. The energy consumed by the three-motor powertrain is compared with the consumption of the single-motor system. The energy saved, as well as the increased performance of the new powertrain, are analyzed.

2. ENTRY DATA FOR THE STUDY

2.1 INITIAL CONFIGURATION OF THE VEHICLE

A vehicle configuration with a single motor is used to perform an initial study. For simplification, the mechanical transmissions presented in [20], which are used in the current model, are considered to have no losses.

2.2 VEHICLE AND MOTOR DATA

A vehicle mass of 400 kg having a wheel radius of 0.3 m is considered for the investigations. The vehicle's frontal area is 0.95 m^2, and the aerodynamic drag coefficient is 0.46. In [34] is explained how the speed profile of the testing cycle is transformed into a tractive effort profile required for the powertrain. The tractive effort coefficient is considered 0.8, enabling the calculation of the maximum tractive effort supported by the wheels when conserving the ground adherence. The rolling resistance coefficient, 0.013, helps calculate the rolling resistance force. The operating points to be covered by the powertrain are generated in the torque-speed plane [20]. The same motor as in [41] is used for the current investigations.

Table 1

Characteristics of the motor

Rated / Maximum Power	3 / 5.4 kW
Voltage supply	72 V
Number of pair poles	16
Rated / Maximum current	68 / 136 A
Transmission rapport motor to wheel	1
Torque constant	0.78 Nm/A
Phase Resistance	0.027 Ω
Phase Inductance	0.15 mH
Equivalent static torque	0.89 Nm
Equivalent coefficient of viscous friction	0.021 Nms

[1,2] Electrical Machines, Materials, and Drives, Electrical Engineering Faculty, POLITEHNICA University of Bucharest, Romania, E-mail: liviu_p@yahoo.com, ocraiu@yahoo.com

3. SINGLE-MOTOR POWERTRAIN

3.1 OPERATIONAL AREA COVERAGE

A normalized testing cycle, WLTC, is used to perform the investigations. The corresponding speed profile is presented in Fig. 1.

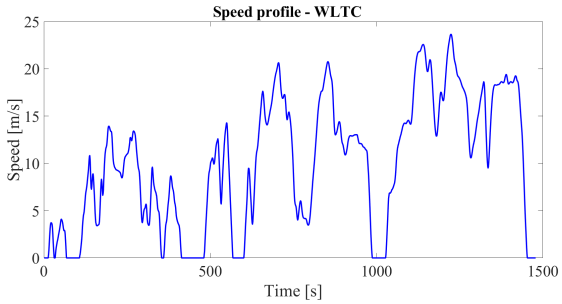

Fig. 1 – Testing cycle speed profile.

For a given speed of the vehicle, the powertrain's necessary torque using MATLAB-Simulink blocks is shown in Fig. 2.

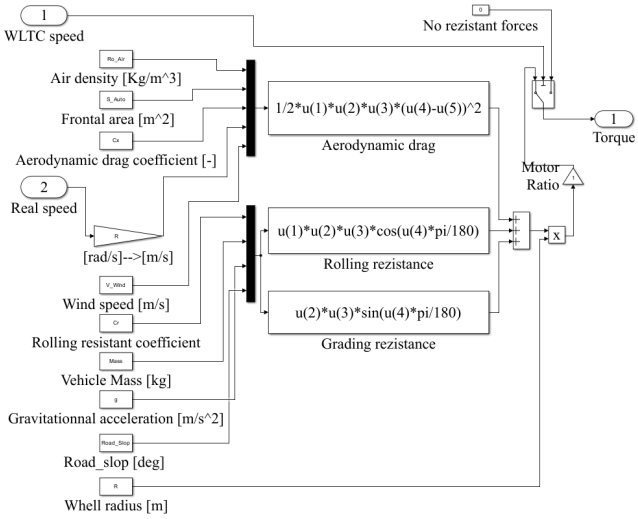

Fig. 2 – Resistant torque for a given speed.

To determine the total torque requirement, vehicle inertia must also be considered. The inertial torque is computed as the product between the vehicle mass, acceleration, and wheel radius (the transmission ratio motor to the wheel is 1). The vehicle's acceleration is computed from the speed profile at each operating point.

From the motor's data is possible to determine the theoretical mechanical characteristic, which is then limited by the maximum torque (restricted by the maximum supplied current) and maximum power (motor-rated power) supported by the motor – represented with the black dashed lines in Fig. 3, the blue dashed line corresponding to the motor nominal torque.

Based on experimental measurements and simulations, a more realistic mechanical characteristic is obtained – represented with solid lines in the next figure. The black line represents the maximum torque variation against the speed. Figure 3 shows that a single motor can move the vehicle with limited acceleration and a maximum speed smaller than the required speed.

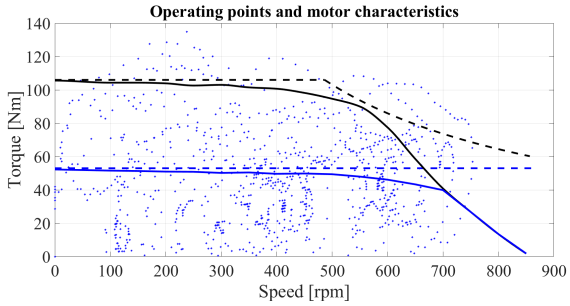

Fig. 3 – Motor mechanical characteristics and required operating points.

3.2 MOTOR LOSSES

Not all the electrical power received by the motor is transformed into mechanical power. A first fraction, P_J, is dissipated as Joule losses in the motor's windings, as the product between the windings' resistance and the square of the current passing through the windings. The remaining power is the electromagnetic one:

$$P_E = P_{el} - P_J. \quad (1)$$

The electromagnetic torque is given by:

$$T_E = P_E / \Omega, \quad (2)$$

where Ω [rad/s] is the angular speed of the rotor.

The second fraction of the power losses are the iron losses:

$$P_{iron} = P_E - P_{shaft}, \quad (3)$$

where, P_{shaft}, is the mechanical power produced by the motor. The iron losses, P_{iron}, have two components, one representing hysteresis losses that depend on the angular speed and the other, the eddy current losses, which are proportional to the square of the angular speed:

$$P_{iron} = (T_{f0} + F_v \cdot \Omega) \cdot \Omega, \quad (4)$$

The hysteresis and eddy current losses are equivalent to T_{f0}, the equivalent static torque, and a viscous torque, respectively. F_v is the viscous friction coefficient provided in the motor characteristics. The methodology for computing these coefficients presented in [34] was implemented using MATLAB. The power losses are represented in Fig. 4-6.

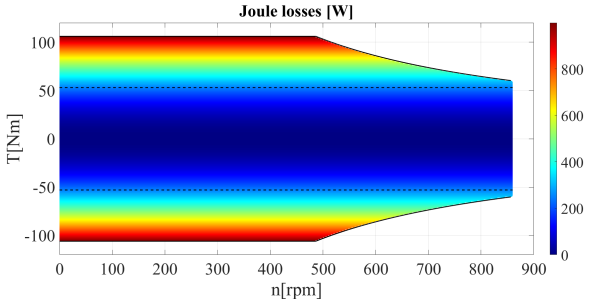

Fig. 4 – Joule losses are represented in the speed–torque plan.

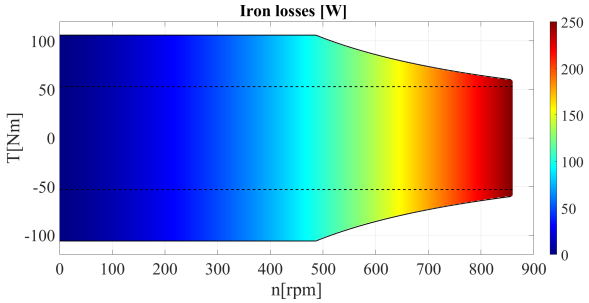

Fig. 5 – Iron losses represented in the speed–torque plan.

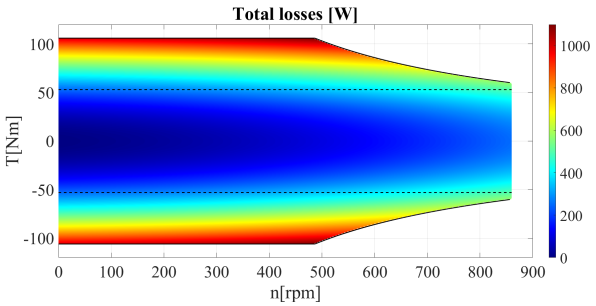

Fig. 6 – Total losses represented in the speed–torque plan.

From the above figures, for the studied motor (but also, in general, for any other motor), it appears that the Joule losses have the greatest weight. As they are proportional to the square of the motor current, reducing the motor current is an important way to enhance the vehicle's energy efficiency.

3.3 EFFICIENCY MAP

There are three ways to generate the motor efficiency map: analytic calculations, simulations, or experimental measurements [20]. A more accurate result is obtained by using the last two methods. However, conducting experimental measurements and performing the needed simulations can take time, and thus results are reduced to several points. Therefore, combining the data from both methods and using interpolation is a good way to reduce the effort in determining the efficiency map.

Figure 7 presents the chart of the process used to generate the motor efficiency map shown in Fig. 8. The highest motor efficiency is obtained by keeping the motor under its nominal torque (marked with a blue line in Fig. 8).

However, in real life, an EV powertrain must provide instant torque bursts or high speeds, which means the motor does not always operate under its rated torque or at points of high efficiency. Therefore, a more important analysis is how much electric power the motor uses during a driving cycle.

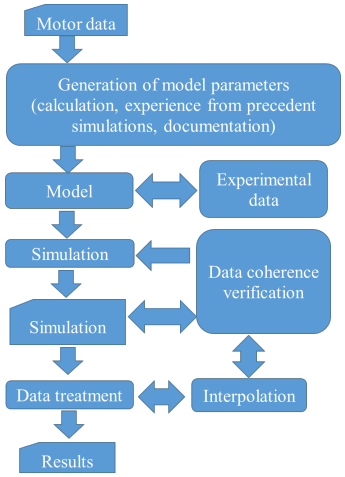

Fig. 7 – The algorithm chart for computing the motor efficiency map.

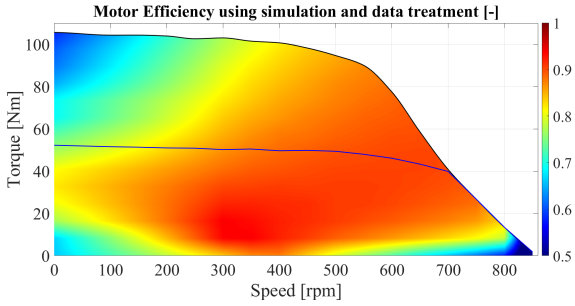

Fig. 8 – Resulting efficiency map of the motor.

3.4 ENERGY EFFICIENCY

To investigate the vehicle's efficiency using the electric powertrain, a MATLAB/Simulink model was developed, Fig. 9. The WLTC speed profile from Fig. 1 is used as entry data. By ″Speed treatment″ block, the imposed vehicle and motor speed are calculated.

.

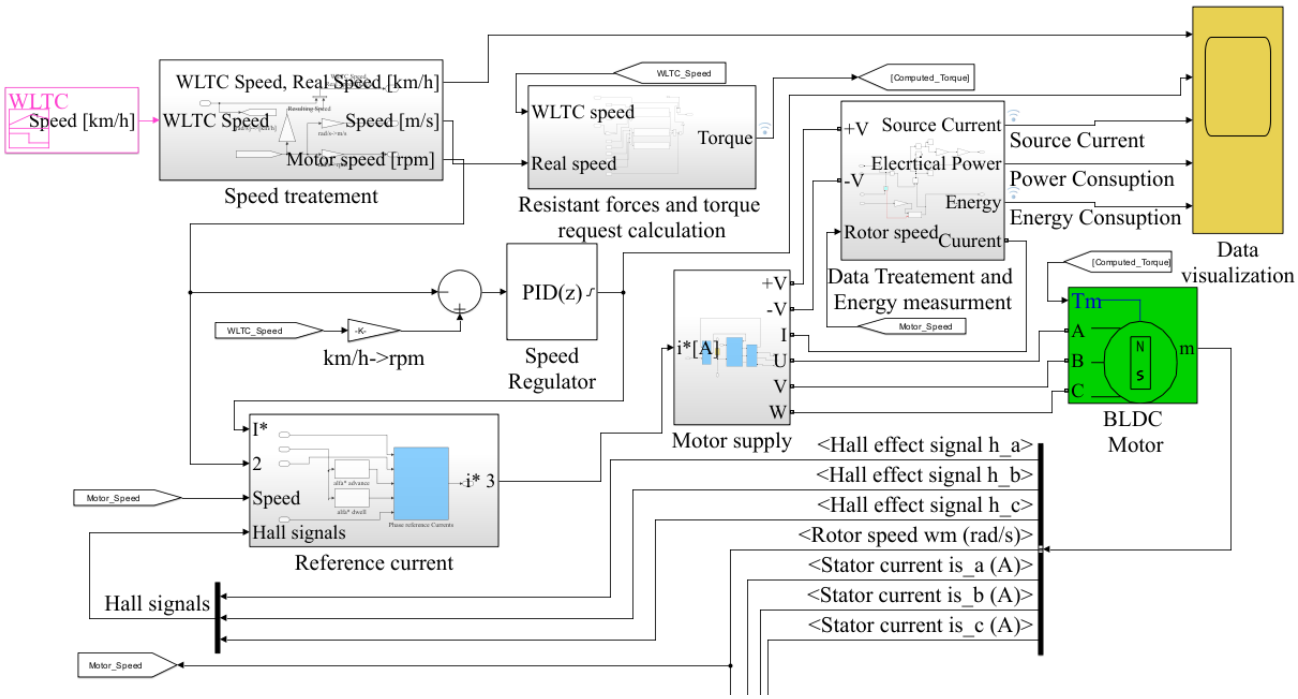

Fig. 9 – MATLAB/Simulink model for energy efficiency investigations.

The block ″Resistant forces and torque request calculation″ is already shown in Fig. 2. A PID regulator imposes a reference current transformed by the block with the same name in three reference currents (one for each motor phase) supplied to the motor. The consumed electric energy is calculated by ″Data Treatment and Energy measurement″ block.

To complete the study, the high-speed zone of the WLTC was used. That corresponds to the time interval between 1000 and 1500 seconds of the speed profile shown in Fig. 1. The energy consumed during this high-speed zone of the powertrain using a single motor is taken as a reference. The evolution of the energy consumption of the single-motor powertrain is shown in Fig. 10.

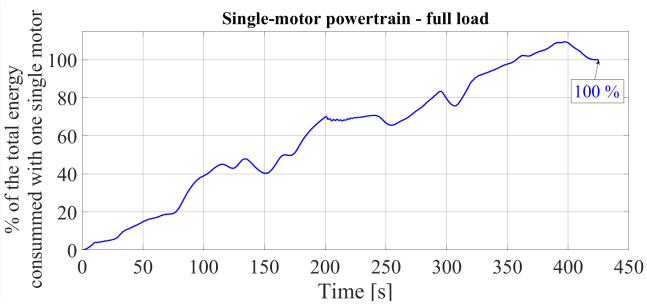

Fig. 10 – Energy consumed with a single-motor powertrain as reference for the study.

4. ENERGY EFFICIENCY WITH THE THREE-MOTOR POWERTRAIN

Analyzing the high-speed zone of the testing cycle, it results in a mean traction torque of 51.67 Nm for the area of the efficiency map placed under the rated theoretical torque (computed as the product between the rated current and motor torque constant). The mean braking torque corresponding to the same region is 48.83 Nm. This confirms that one single motor could move the vehicle with reduced performance.

Figure 3 shows that a powertrain with three identical motors will better cover the request. The new vehicle configuration is proposed in Fig. 11.

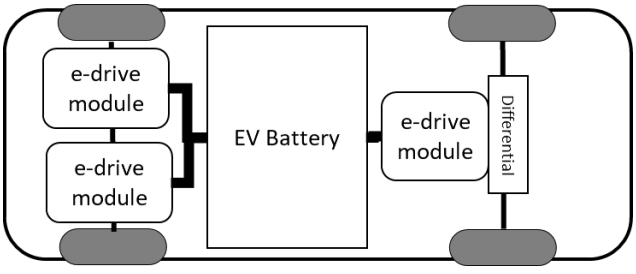

Fig. 11 – Vehicle configuration with a three-motor powertrain.

As in any EV, mechanical stability comes first, and it is not possible to split the total required torque between motors only by using the energy optimization criteria discussed above.

A static load allocation is considered for all high-speed energy measurement zones. The frontal axle should cover 40 % of the necessary torque using a single motor, while the remaining 60 % of the torque is provided by the other two motors at the rear axle.

From the frontal motor, the evolution of the consumed energy reported to the reference energy is shown in Fig. 12. Finally, in the new configuration, the frontal motor producing 40 % of the requested torque consumes less than 40 % of the reference energy.

The energy consumption of the front motor, referred to in the reference energy chart in Fig. 10, is shown in Fig. 12. As it can be seen, in this new configuration, the motor on the front shaft produces 40 % of the needed torque and consumes 32.83 % of the reference energy.

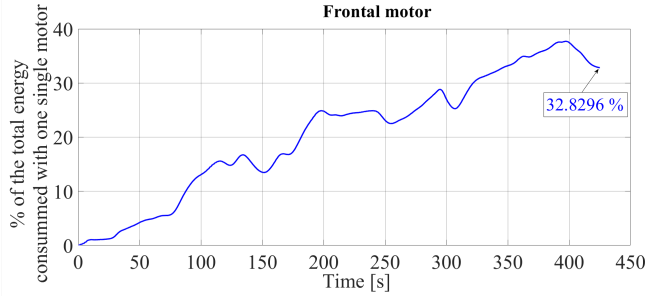

Fig. 12 – Energy evolution for the frontal motor – static load allocation (60 % on rear axle, 40 % on front axle).

A similar result is obtained for rear motors producing each 30 % of the requested torque while consuming only 22.98 % of the reference energy, Fig. 13.

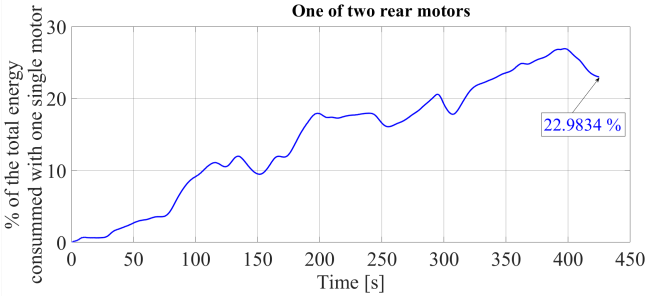

Fig. 13 – Energy evolution for one of the rear motors– static load allocation (60 % on rear axle, 40 % on front axle).

The best efficiency with this powertrain is obtained for an optimal load repartition among the motors [29]. In the case of a powertrain with three identical motors, the optimal efficiency is obtained when each motor produces one-third of the total torque. The time evolution of the energy consumption of a single motor when it produces one-third of the required torque (i.e., at optimal load repartition), is shown in Fig. 14.

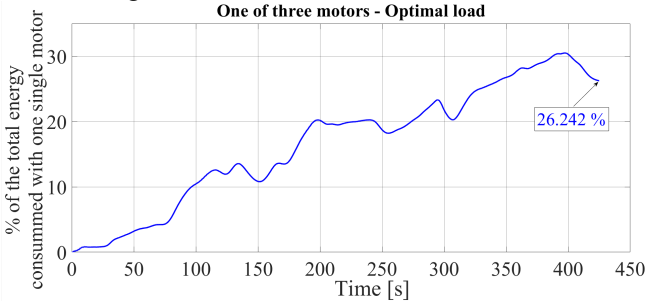

Fig. 14 – Energy evolution for one of the rear motors– optimal load allocation (one-third on each motor).

For the proposed powertrain with three motors, the resulting energy consumption when the vehicle operates at a high-speed area of the WLTC, and a 40 % - 60 % load

repartition, is reduced by 21.2036 % compared to the reference energy consumption.

When an optimal load repartition is considered (one-third of the load on each of the motors), the consumed energy is smaller by 21.2739 % than the reference energy consumption. It results that for the individual motor of the powertrain, being in a three identical motors configuration, the optimal load repartition doesn't significantly increase the saved energy, and a 40 % - 60 % load repartition gives satisfaction.

That means the efficiency of the proposed powertrain with three identical motors does not significantly increase when the optimal load repartition applies (one-third of load on each motor) compared to a 40 % - 60 % load distribution between the front and rear axle. Depending on running conditions, such an uneven load repartition between the front and the rear axle is specific to vehicles having a four-wheel drive system, offering better traction capabilities and increasing energy efficiency.

11. **CONCLUSIONS**

A three-identical motor powertrain for an EV has been investigated from the energy consumption point of view. The results were compared with those obtained for a single-motor powertrain.

Using three instead of one motor in the new topology powertrain generates enhanced acceleration, maximum speed, and maximum torque performance. Simultaneously, using three motors allows important energy savings compared to energy consumption when only one motor is used.

In the coverage of the operating points with multiple motors, the knowledge of the efficiency map of the individual motor is an important element in establishing the number of motors and the configuration of the powertrain.

As the load repartition between motors must first satisfy a vehicle stability criterion, there is possible to generate an enhanced energy efficiency by the configuration of the powertrain. For the investigated case, a 40 % - 60 % load repartition between vehicle axles gave similar savings to an optimal load repartition between the powertrain motors.

ACKNOWLEDG(E)MENT(S)

Special thanks for supporting this research and for assisting in the development of a multi-motor didactic platform, Fig. 15, are addressed to the Department of Electrical Machines, Materials, and Drives in the Electrical Engineering Faculty, of the Polytechnic University of Bucharest.

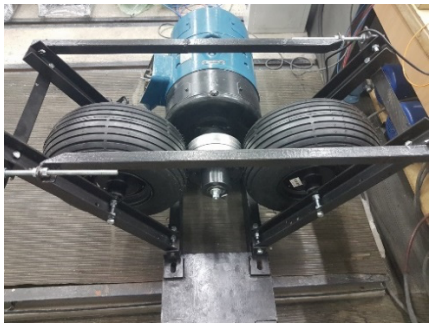

Fig. 15 – Platform with two in-wheel motors and a dc generator operating as load.

Received on 29 January 2023

REFERENCES

1. L. Popescu, *Electromobility topics entering a new decade*, Electric machines, materials and drives present and trends (SME 2020), APME, **16**, *1*, pp. 131–140 (2020).
2. M.V. Castro et al., *A review of existing multi-motor electric powertrain sizing strategies*, 2021 24th International Conference on Electrical Machines and Systems (ICEMS), pp. 2419–2424 (2021).
3. S. Cui, S. Ha, C.C. Chan, *Overview of multi-machine drive systems for electric and hybrid electric vehicles*, 2014 IEEE Conference and Expo Transportation Electrification Asia-Pacific (ITEC Asia-Pacific), pp. 1–6 (2014).
4. L. Popescu, L. Dumitran, A. Stanescu, *Multi-motor solutions for electric vehicles*, 2021 International Conference on Applied and Theoretical Electricity (ICATE), pp. 1–6 (2021).
5. Y. Xu, Z. Cheng, W. Tang, *Design of Multi-motor Synchronous Control System,* 2021 3rd Asia Energy and Electrical Engineering Symposium (AEEES), pp. 846–851 (2021).
6. O. Craiu, T. I. Ichim, L. M. Melcescu, L. Popescu, *Optimization of a high torque density small hybrid stepper using 3D FEM model*, International Symposium on Power Electronics, Electrical Drives, Automation and Motion (SPEEDAM), pp. 610–615 (2022).
7. O. Nezamuddin, R. Bagwe, E. Dos Santos, *A Multi-Motor Architecture for Electric Vehicles*, IEEE Transportation Electrification Conference and Expo (ITEC), pp. 1–6 (2019).
8. M.D. Jahnke, A.M. Miguel, J.P. Rastelli, P.A. Pablo, A.M. Sandi, *Multi motor electric powertrains: Technological potential and implementation of a model based approach*, IECON, 42nd Annual Conference of the IEEE Industrial Electronics Society, pp. 223–228 (2016).
9. L. Popescu, A. Stănescu, Șt. Vasiliu, *Didactical platform for multi-motor solutions*, in Electric machines, materials and drives present and trends (SME 2021), APME, **17**, *1*, pp. 172–180 (2021).
10. A. Rassolkin, H. Heidari, A. Kallaste, T. Vaimann, J.P. Acedo, E. Romero-Cadaval, *Efficiency map comparison of induction and synchronous reluctance motors*, 26th International Workshop on Electric Drives: Improvement in Efficiency of Electric Drives (IWED), pp. 1–4 (2019).
11. H. Sano, K. Semba, Y. Suzuki, T. Yamada, *Investigation in the accuracy of FEA Based Efficiency Maps for PMSM traction machines*, 2022 International Conference on Electrical Machines (ICEM), pp. 2061–2066 (2022).
12. S. Stipetic, J. Goss, *Calculation of efficiency maps using scalable saturated flux-linkage and loss model of a synchronous motor*, XXII International Conference on Electrical Machines (ICEM), pp. 1380–1386 (2016).
13. H.-C. Jung, D.-J. Kim, S.-Y. Jung, D. Lee, *Optimization method to maximize efficiency map of a drive motor with electrical winding changeover technique for hybrid EV*, IEEE Transactions on Applied Superconductivity, **30**, *4*, pp. 1–5 (2020).
14. H. Sano et al., *Loss analysis of a permanent magnet traction motor in a finite element analysis based efficiency map*, International Conference on Electrical Machines (ICEM), pp. 2301–2306 (2020).
15. M.H. Mohammadi, D.A. Lowther, *A computational study of efficiency map calculation for synchronous ac motor drives including cross coupling and saturation effects*, IEEE Conference on Electromagnetic Field Computation (CEFC), pp. 1 (2016).
16. L. Song, Z. Li, Z. Cui, G. Yang, *Efficiency map calculation for surface-mounted permanent-magnet in-wheel motor based on design parameters and control strategy*, IEEE Conference and Expo Transportation Electrification Asia-Pacific (ITEC Asia-Pacific), pp. 1–6 (2014).
17. T. Tudorache, A. Marinescu, A. Vintilă, *Inductive coupler for battery charging system of heavy electric vehicles*, Rev. Roum. Sci. Techn. – Électrotechn. Et Énerg., **68**, *1*, pp. 71–76 (2023).
18. J.G. Malar et al., *Electric vehicle onboard charging via harris hawks optimization-based fractional-order sliding mode controller*, Rev. Roum. Sci. Techn. – Électrotechn. Et Énerg., **68**, *1*, pp. 30–35 (2023).
19. T. Roubache, S. Chaouch, *Nonlinear fault tolerant control of dual three-phase induction machines based electric vehicles*, Rev. Roum. Sci. Techn. – Électrotechn. Et Énerg., **68**, *1*, pp. 65–70 (2023).

20. L. Popescu, A. Stănescu, *Efficiency maps for an EV BLDC motor using analytic calculation and simulation*, in Electric machines, materials and drives present and trends (SME 2022), APME, **18**, *1*, pp. 89–99 (2022).
21. G. Haines, N. Ertugrul and W. L. Soong, *Autonomously obtaining system efficiency maps from motor drive systems*, IEEE International Conference on Industrial Technology (ICIT), pp. 231–236 (2019).
22. S. M. Lukic, A. Emado, *Modeling of electric machines for automotive applications using efficiency maps*, Proceedings: Electrical Insulation Conference and Electrical Manufacturing and Coil Winding Technology Conference (Cat. No.03CH37480), pp. 543–550 (2003).
23. J. Brousek, L. Krcmar, P. Rydlo, *Efficiency measuring of electric drive with traction synchronous motor with permanent magnets*, IEEE International Workshop of Electronics, Control, Measurement, Signals and their application to Mechatronics (ECMSM), pp. 1–5 (2021).
24. S. Stipetic, J. Goss, D. Zarko, M. Popescu, *Calculation of efficiency maps using a scalable saturated model of synchronous permanent magnet machines*, IEEE Transactions on Industry Applications, **54**, *5*, pp. 4257–4267 (2018).
25. L. Popescu, L. Melcescu, O. Craiu, A. Craciunescu, V. Bostan, *Phase advance, and dwell control applied to a pm BLDC motor for increasing the maximum speed of an electric vehicle*, International Symposium on Power Electronics, Electrical Drives, Automation and Motion (SPEEDAM), pp. 850–855 (2022).
26. B. Kuznetsov, I. Bovdui, T. Nikitina, V. Kolomiets, B. Kobilyanskiy, *Multi-motor plant related electric drives robust control synthesis*, IEEE 4th International Conference on Intelligent Energy and Power Systems (IEPS), pp. 242–245 (2020).
27. K. Sharma, A. Agrawal, S. Bandopadhaya, S. Roy, *Fuzzy logic based multi motor speed control of electric vehicle*, IEEE 5th International Conference for Convergence in Technology (I2CT), pp. 1–5 (2019).
28. F. Gustin, A. Berthon, *Simulation of a multi-motor soft switching converter for electric vehicle application*, Proceedings IPEMC Third International Power Electronics and Motion Control Conference (IEEE Cat. No.00EX435), **2**, pp. 660–664 (2000).
29. L. Popescu, L. Melcescu, L. Dumitran, A. Crăciunescu, *Analysis of the influence of wheel torque distribution on energy efficiency in the case of an electric vehicle with two motors* [abstract], in Proceeding book of 1st International Conference on Applied Engineering and Natural Sciences (ICAENS), Konya, Turkey, pp. 300 (2021).
30. M.V. Castro et al., *Non–dominated sorting genetic algorithm based determination of optimal torque–split ratio for a dual–motor electric vehicle*, IECON47th Annual Conference of the IEEE Industrial Electronics Society, pp. 1–6 (2021).
31. R. de Castro, R. E. Araujo, H. Oliveira, *Design, development and characterisation of a FPGA platform for multi-motor electric vehicle control*, IEEE Vehicle Power and Propulsion Conference, pp. 145–152 (2009).
32. D.V. Volkov, Y.P. Stashinov, *Equalization of torques in multi-motor electric drives with estimation of motors parameters*, International Multi-Conference on Industrial Engineering and Modern Technologies (FarEastCon), pp. 1–5 (2018).
33. S. Cui, S. Han, C.C. Chan, *Overview of multi-machine drive systems for electric and hybrid electric vehicles*, IEEE Conference and Expo Transportation Electrification Asia-Pacific (ITEC Asia-Pacific), pp. 1–6 (2014).
34. L. Popescu, L. Melcescu, L. Dumitran, A. Crăciunescu, A. Stănescu, *Control analysis of a bi-motor electric traction system for energy and performance optimization*, International Scientific Conference on Communications, Information, Electronic and Energy Systems (CIEES), 2021, AIP Conference Proceedings, **2570**, *040002* (2022).
35. M. Pechinik, M. Pushkar, S. Burian, L. Kazmina, *Investigation of energy characteristics of the electromechanical system in multi-motor conveyors under variation of traction load level on the belt*, IEEE 6th International Conference on Energy Smart Systems (ESS), pp. 303–306 (2019).
36. Ž. Ferková, P. Bober, *Magnetic shield optimization for the multi-motor assembly*, APME, pp. 1–4 (2017).
37. L. Mo, *Power balance control of multi-motor driving using double fuzzy controller*, IEEE International Conference on Intelligent Computing and Intelligent Systems, pp. 67–70 (2010).
38. C.L. Popescu, L.M. Dumitran, A. Stănescu, *Simulation of multi-motor propulsion system for energy efficiency in electric vehicles* in Annals of the University of Craiova, Electrical Engineering series, **45**, *1*, pp 75–82 (2021).
39. J. Lemmens, J. Driesen, *Synchronization and efficiency analysis of a direct-drive multi-motor application*, 6th IET International Conference on Power Electronics, Machines, and Drives (PEMD 2012), pp. 1–6 (2012).
40. X. Sun et al., *MPTC for PMSMs of EVs with multi-motor driven system considering optimal energy allocation*, in IEEE Transactions on Magnetics, **55**, *7*, pp. 1–6, (2019).
41. L. Popescu, L. Melcescu, O. Craiu, *Energy efficiency improvement for an electric vehicle PM BLDC propulsion system using phase advance and dwell control*, International Conference on Electrical, Computer, Communications and Mechatronics Engineering (ICECCME), pp. 1–6 (2022).